Whitmarsh, R.B., Sawyer, D.S., Klaus, A., and Masson, D.G. (Eds.), 1996
Proceedings of the Ocean Drilling Program, Scientific Results, Vol. 149

39. SEISMIC STRATIGRAPHY AND TECTONIC HISTORY OF THE IBERIA ABYSSAL PLAIN[1]

R.C.L. Wilson,[2] D.S. Sawyer,[3] R.B. Whitmarsh,[4] J. Zerong,[3] and J. Carbonell[5]

ABSTRACT

This paper presents an interpretation of seismic reflection profiles acquired in the southeastern part of the Iberia Abyssal Plain using lithostratigraphic and biostratigraphic information obtained from ODP Leg 149 and DSDP Site 398. Six seismic units are recognized; Units 1 to 5 span the lower Albian to Holocene, but some doubt exists concerning the age of Unit 6; it is probably Valanginian to Aptian in age.

Only seismic Units 1 and 2 are not deformed significantly by a previously identified Neogene compressional episode. Unit 2 onlaps the folds, and Unit 1 truncates them in places and oversteps Unit 2 toward the fold crests. The boundary between Units 2 and 3 coincides with the late/middle Miocene boundary and so constrains the main compressional event to a very short period of time. Undulatory and inclined reflections in Units 1-3 indicate significant sediment transport by contour currents since the middle Eocene. Depressions between acoustic basement highs were filled by sediments equivalent to Units 4-6, commencing in the Early Cretaceous (probably during the Valanginian). The sedimentary fill shows simple onlapping relationships with the flanks of basement highs, most of which were completely sediment covered by Eocene time.

Applying accepted criteria for the recognition of synrift packages on seismic sections, we found no unequivocal examples of synrift intervals in the study area or on previously published seismic sections from the deep Galicia Margin. Therefore, we conclude that the rift episode affecting the western Iberian Margin, from the Iberia Abyssal Plain northward, occurred over a very short interval, and/or that depositional rates were very low, so that synrift sedimentary sequences did not accumulate to produce a seismically resolvable thickness. The results of this study strongly suggest that rifting on the southeastern margin of the Iberia Abyssal Plain occurred at the latest before the Hauterivian, probably early in the Valanginian and after the Tithonian. We suggest that the synrift episode beneath the deep Galicia Margin postdates Tithonian-Berriasian shallow-water carbonates and predates Valanginian siliciclastic sediments that infill the basement topography created during rifting.

Unfortunately, almost no in situ sediments were obtained from Leg 149 sites that would have enabled paleodepth estimates to be made for the Cretaceous. Therefore, it was not possible to quantify tectonically driven postrift subsidence. However, using digitized versions of the interpreted seismic lines, smoothed total tectonic subsidence (TTS) plots along these lines were produced, from which crustal thickness and extension factors (β) were determined. TTS of up to 6 km is consistent with the subsidence of either normal oceanic crust formed ≥ 100 Ma or continental crust thinned by (β of between 5 and 7 at 135 Ma.

INTRODUCTION

The first part of this paper summarizes the seismic stratigraphy recognized in the Ocean Drilling Program (ODP) Leg 149 area and its relationship to lithostratigraphic and biostratigraphic data obtained at Sites 897-900 and Deep Sea Drilling Project (DSDP) Site 398. The second part presents three approaches to understanding the tectonic history of the area: (1) seismic stratigraphic evidence for the timing of rifting, (2) subsidence at individual Leg 149 sites, and (3) total tectonic subsidence (TTS) based on digitized versions of the interpreted seismic lines.

Figure 1 shows the location of the seismic lines interpreted during this study and the positions of DSDP Site 398 and ODP Sites 897-901. Data from the following seismic surveys were used:

Data type	Survey name	Acquisition date
Single channel	*Discovery* 161	1986
	JOIDES Resolution 149	1993
24-fold stacked and migrated	*Lusigal* (LG)	1990
	Sonne 75 (SO)	1991

A variety of problems was faced when interpreting the data. Differing acquisition and processing methods (including the fact that the *Lusigal* and *Sonne* lines were not processed in the same way) result in differing reflection characteristics (i.e., seismic facies) displayed by the same stratigraphic intervals on adjacent lines. Correlation across basement highs is problematic for two reasons. First, onlap onto the highs made it impossible to correlate individual reflections or reflection packages from one low to the next along the same line unless they could be tied together along other parts of the seismic grid; given the relatively wide spacing of the lines (Fig. 1), this was rarely possible. Second, compressional structures (folds and faults) above some basement highs made it difficult to trace reflections over and across them, although it was generally possible to trace them around other parts of the grid.

At the start of the study, no attempt was made to recognize the seismic stratigraphic units defined in adjacent areas by earlier workers (Groupe Galice, 1979; Mauffret and Montadert, 1988). The bases of six reflection packages were identified using a combination of reflection terminations and/or reflection characteristics. In areas where the bases of seismic units could not be recognized using such criteria,

[1]Whitmarsh, R.B., Sawyer, D.S., Klaus, A., and Masson, D.G. (Eds.), 1996. *Proc. ODP, Sci. Results,* 149: College Station, TX (Ocean Drilling Program).
[2]Department of Earth Sciences, Open University, Milton Keynes, MK7 6AA, United Kingdom. R.C.L.Wilson@open.ac.uk
[3]Department of Geology, Rice University, P.O. Box 1892, Houston, TX 77251, U.S.A.
[4]Institute of Oceanographic Sciences Deacon Laboratory, Brook Road, Wormley, Surrey GU8 5UB, United Kingdom. Present address: Challenger Division for Seafloor Processes, Southampton Oceanography Centre, Empress Dock, European Way, Southampton SO14 3ZH, United Kingdom.
[5]Institute of Earth Sciences, Jaume Almera, Lluis Sole i Sabaris s/n, 08028 Barcelona, Spain.

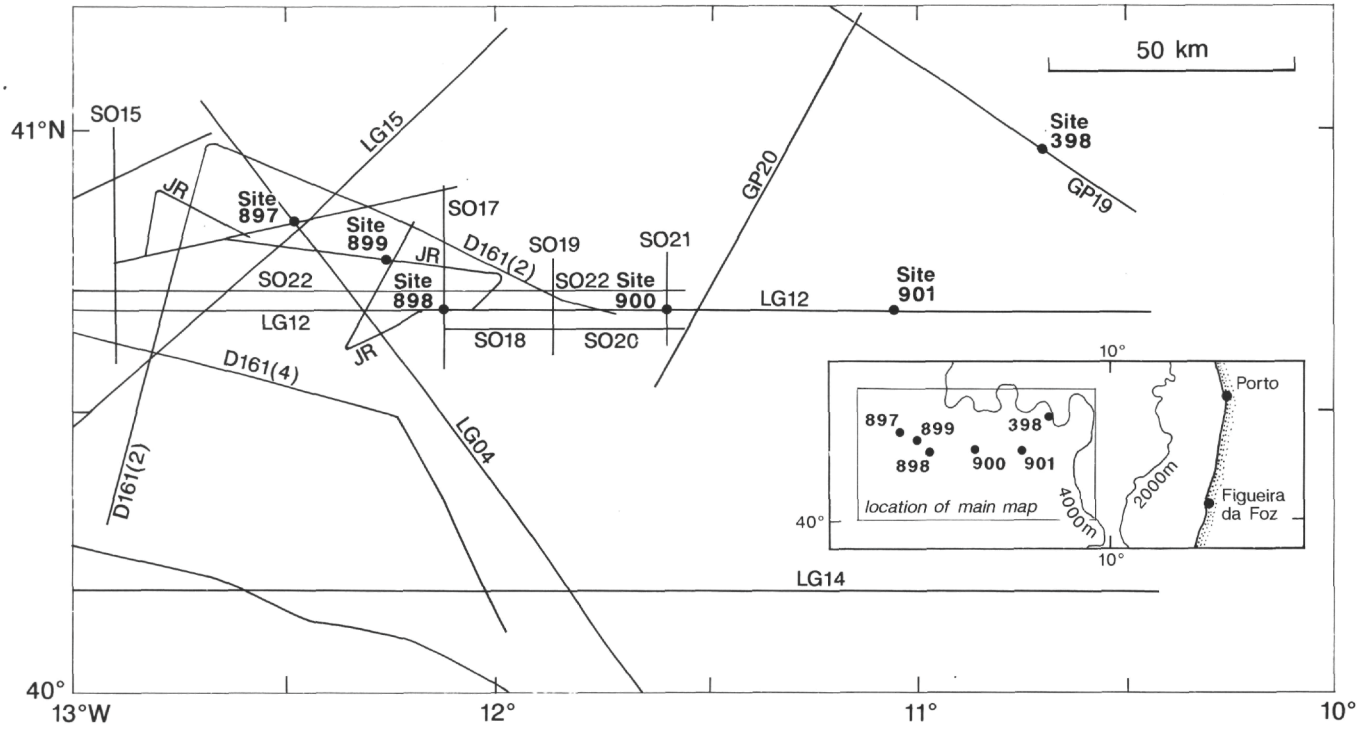

Figure 1. Map showing the location of seismic lines interpreted during this study and the Leg 149 (897-901) and DSDP Leg 48B (398) drilling sites. D = *Discovery* lines; JR = *JOIDES Resolution* lines; LG = *Lusigal* lines; SO = *Sonne* lines. The location of lines GP19 and GP20 is shown to demonstrate how interpretations in this study were linked to those of Groupe Galice (1979); extracts from these lines are shown in Figures 7 and 10.

they were located by tracing the boundaries around the seismic grid from the parts of profiles where the criteria for boundary recognition are clear.

The seismostratigraphic boundaries we recognized were equated to the lithostratigraphy and biostratigraphy determined at Sites 897-900 by converting depths in two-way traveltime to depths in the holes using the sonobuoy-based velocity structure of Whitmarsh et al. (1990b). These data provided very accurate (±20 m) depth estimates to basement during Leg 149.

The deepest borehole penetration (750 m) of the layered reflection sequence was achieved at Site 900, equivalent to 800 ms two-way traveltime (TWT). This is barely one-third of the maximum depth in time of 2200 ms TWT observed in the study area and probably represents only one-quarter of the maximum thickness of sediments overlying acoustic basement (which is probably greater than 2.7 km). Therefore, biostratigraphic and lithostratigraphic data obtained during Leg 149 only illuminate the age and sedimentary character of seismic stratigraphic Units 1-3 and the upper part of Unit 4. Comparisons to the sequence drilled at DSDP Site 398 enable suggestions to be made concerning the age and likely lithologic character of sediments equivalent to the remainder of Unit 4 and to Units 5 and 6.

The foldout sheet enclosed in the back pocket of this volume includes a map (Fig. 2, back pocket) that shows the location of folds described by Masson et al. (1994) and line drawings of our interpretation of profiles LG04, LG12, SO16-18, and SO20. Figure 1 of Beslier (this volume), a reproduction of almost the entire length of profile LG12, also can be found as a foldout in the back pocket.

SEISMIC UNITS

Units 1 and 2

The geometry of Units 1 and 2 is related to large-amplitude asymmetric folds described by Masson et al. (1994); the location of these structures is shown in Figure 2 (back-pocket foldout). The characteristic features of these units are that Unit 2 onlaps the steeper western side of these folds, whereas Unit 1 occurs as a continuous sheet above them (Fig. 3A-C, back pocket; Figs. 4, 5). The wedge-shaped geometry of Unit 2 is caused by a combination of onlap at its base and erosional truncation at the base of Unit 1, resulting in the absence of Unit 2 over the crests of the folds. The two units cannot be distinguished from one another to the east of Site 898.

Unit 1: Description

The base of Unit 1 is defined in the western part of the study area, where erosional truncation of Units 2 and 3 occurs. Erosional truncation is well displayed in the vicinity of Site 897 on lines SO16 and LG04 (Fig. 3A, B, back pocket; Fig. 4) and to the west of Site 898 on line LG12 at about shotpoint (SP) 2700 at 7200 ms TWT (Fig. 3C, back pocket; Fig. 5). Unit 1 shows a sheetlike geometry, ranging in thickness from less than 100 ms in the east to 270 ms west of Site 897. It is characterized by high-amplitude reflections with moderate to good continuity. East-northeast of Site 897, there is a marked change in reflection amplitude into the underlying Unit 3, in which amplitudes are low (Fig. 4).

Unit 2: Description

The base of Unit 2 is defined by onlap onto the broad asymmetrical anticlinal fold structures affecting Unit 3 and deeper units. Onlap is well displayed to the west of Site 897 on lines SO16 (Fig. 3A, back pocket; Fig. 4) and LG04 (Fig. 3C, back pocket), between Site 898 and SP 2500 on LG12 (Fig. 3C, back pocket; Fig. 5), and at about SP 3000 on SO22. Reflection terminations on the gently dipping east limb of the fold structure enable the base of Unit 2 to be identified on LG04; a minor fault and associated minor folding are truncated by the base of the unit at SP 1595 on this line (Fig. 3B, back pocket).

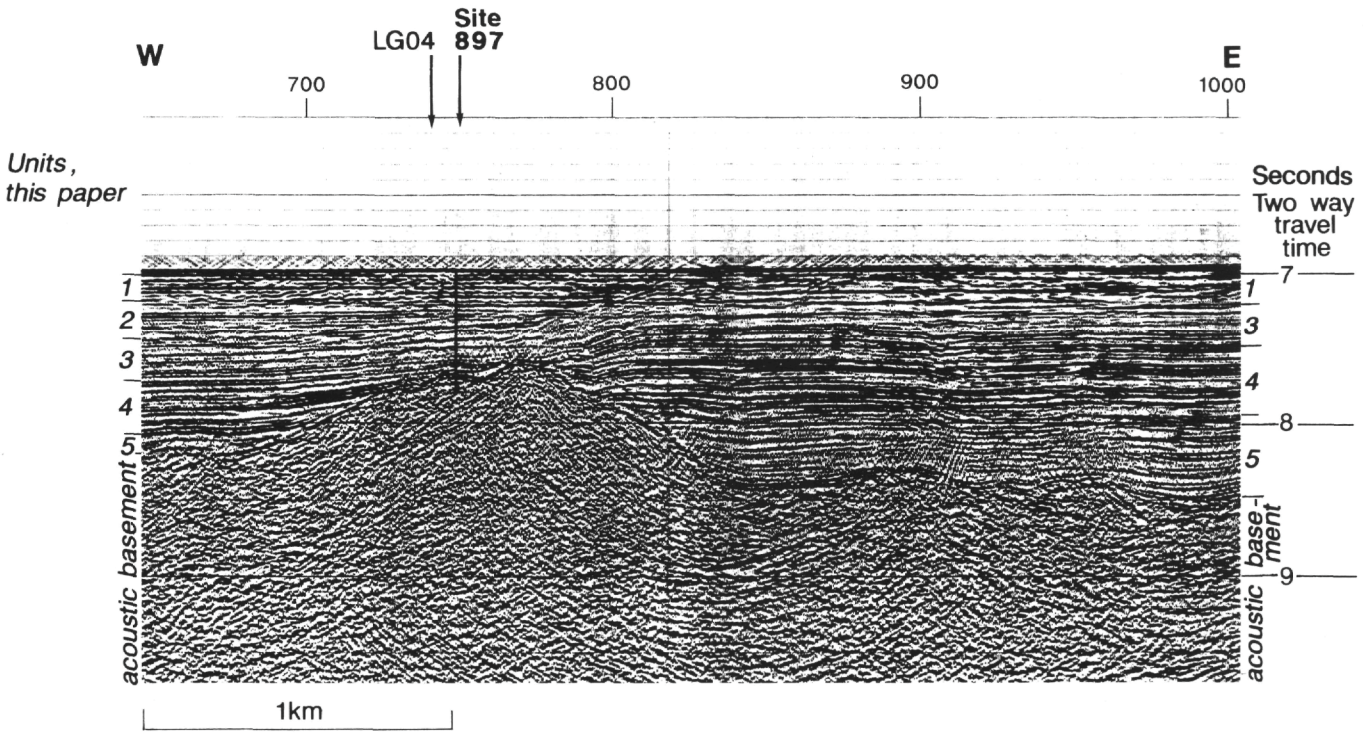

Figure 4. Migrated seismic line *Sonne* 16 across Site 897. For interpretation of this line, see Figure 3A, back pocket. Unit 2 shows onlap onto the flexure affecting older units.

Unit 2 ranges in thickness from 0 to 460 ms, thickening westward away from the folds shown on Figure 2, back pocket. It shows parallel low- to moderate-amplitude reflections to the west of the fold on the *Sonne* lines, but moderate to high amplitude reflections on the *Lusigal* lines. This difference is probably related to different processing parameters.

Units 1 and 2 to the East of Site 898: Description

As previously noted, Units 1 and 2 cannot be mapped separately to the east of Site 898. Unit 1 probably truncates Unit 2 just to the west of Site 898 (Fig. 3C, back pocket). At Site 900, sediments of the same age as those equivalent to Unit 2 at Site 897 were drilled, but it is not possible to distinguish the two units on seismic sections.

To the east of Site 898 on line LG12, low-amplitude (10-20 ms) sediment waves are evident on the seafloor. These, and the wavy reflections within Units 1 and 2, have a wavelength of 1.5 to 2.0 km (Fig. 5). This wavy reflection pattern is not seen on the larger scale *Sonne* lines (SO18, SO20 [Fig. 8], and SO22), which show high-amplitude reflections with low continuity (usually about 0.5-1.5 km long) and a very slightly undulatory pattern beneath mostly parallel reflections near the seafloor. It is difficult to trace the base of Unit 1 through this zone. To the east of Site 900 on LG12 (Fig. 5), the wavy reflection pattern is replaced by parallel to very slightly undulatory, moderate- to low-amplitude reflections. Here, the base of the combined Units 1 and 2 is recognized by reflection terminations (between Site 900 and SP 4100 on LG12; Fig. 3C, back pocket; Fig. 5).

Discussion

Table 1 summarizes information concerning the boundaries of the seismostratigraphic and lithostratigraphic units recognized during Leg 149 (Sawyer, Whitmarsh, Klaus, et al., 1994) and biostratigraphic boundaries and hiatuses identified by de Kaenel and Villa (this volume) at Sites 897-900. Three key points emerge from this information:

1. The boundary between seismic Units 2 and 3 coincides with the early/middle Miocene boundary at Sites 897, 898, and 900.
2. The base of Unit 1 cannot be mapped to the east of Site 898. Between Site 900 and SP 4100 on LG12 (Fig. 3C, back pocket; Fig. 5), a few reflection terminations are recognizable and define the base of the combined Units 1 and 2, as shown on Figure 3C, back pocket. Biostratigraphic information from Site 900 shows that this boundary coincides with the late/middle Miocene boundary. Therefore, we conclude that adjacent to Site 898 (where middle Miocene sediments are only 19 m thick; de Kaenel and Villa, this volume) the base of Unit 1 must truncate Unit 2 toward the crest of the fold. This is consistent with the conclusion of Milkert et al. (this volume) that the later onset of turbidite sedimentation at Site 398 (2.0 Ma compared to 2.6 Ma at Sites 897 and 900) indicates that earlier turbidites may have been eroded.
3. The base of Unit 1 at Sites 897-899 coincides with the base of the upper Pliocene, but at Site 899 it appears to tie with the base of the upper Miocene. This discrepancy is explained by the difficulty of tracing the seismic units on single-channel *JOIDES Resolution* data adjacent to Site 899.

In the light of the above, we conclude that the ages of Units 1 and 2 are

Unit 1: late Pliocene to Holocene;
Unit 2: middle Miocene to late Pliocene.

Unit 1 and the bulk of Unit 2 are equivalent to the turbidite/pelagite sequence described by Milkert et al. (this volume); they suggest that the onset of turbidite sedimentation was caused by a glacioeustatic sea-level fall at 2.6 Ma.

The onlap of reflections within Unit 2 onto the top of Unit 3 constrains the timing of the main pulse of folding to the middle/early Miocene boundary, which is identical to the timing of inversion in the Lusitanian Basin in Portugal (Wilson et al., 1989). This event coin-

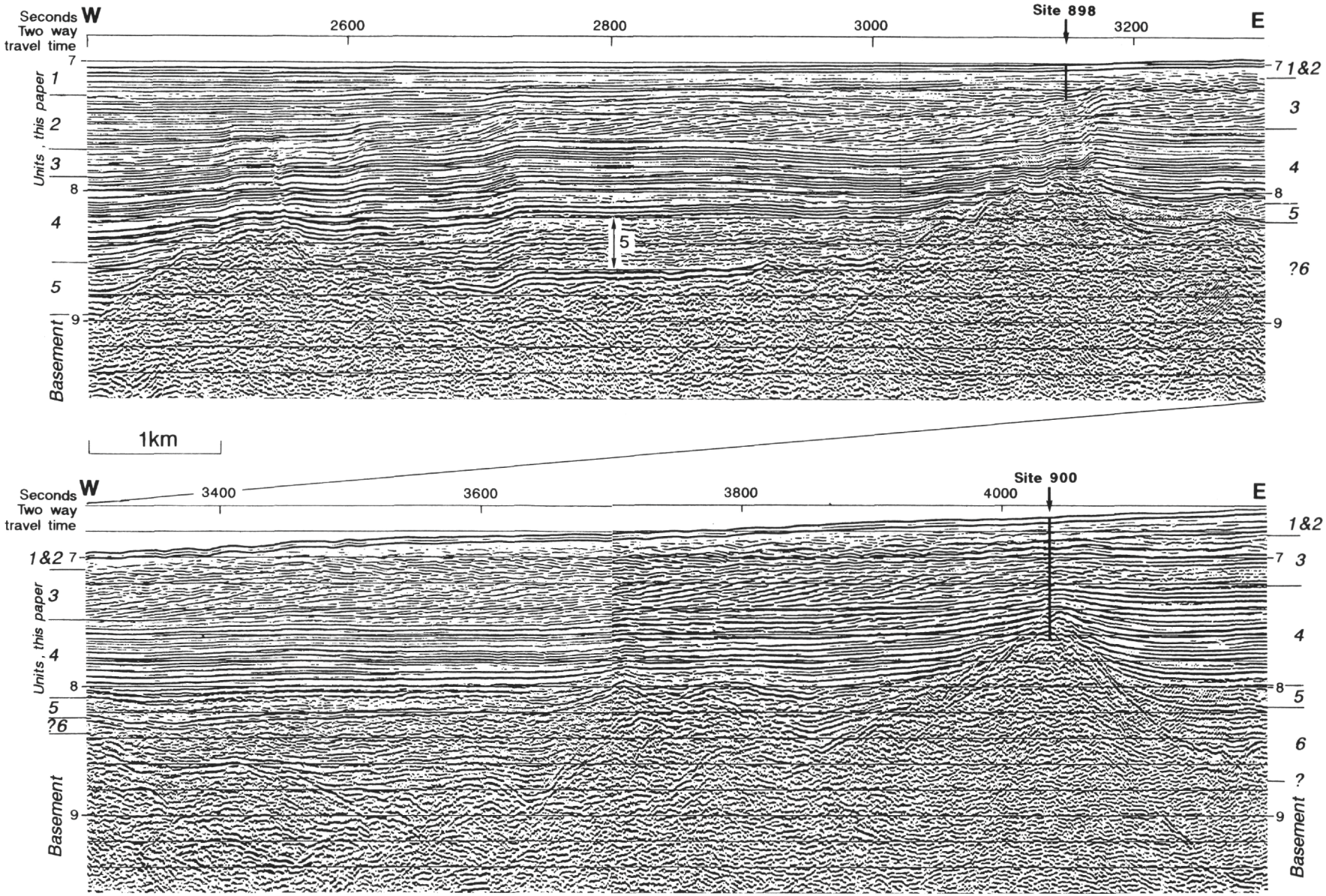

Figure 5. Migrated line *Lusigal* 12 across Sites 898 and 900. For interpretation of this line, see Figure 3C, back pocket. Note (1) the thinning of Unit 2 and its onlap onto Unit 3 toward Site 898, (2) deformation beneath Units 1 and 2 adjacent and to the west of Site 898, (3) the base of the inclined reflection zone between Sites 898 and 900 defines the base of Unit 3, (4) the poor reflection continuity to almost transparent character of Unit 5, and (5) the general westward thickening of this unit (ignoring localized thinning over basement highs).

Table 1. Depth (mbsf) two-way traveltime (ms) beneath seafloor and possible correlations between seismostratigraphic Units 1-3 and depth in biostratigraphy of Leg 149 sites.

Base of Unit	Site 897 (SO 16)				Site 899 (*JOIDES Resolution*)				Site 898 (LG12)				Site 900 (LG)			
		Depths				Depths				Depths				Depths		
	TWT[a]	Computed[b] mbsf	Nearest feature[c]	Age and lithostratigraphy[d]	TWT[a]	Computed[b] mbsf	Nearest feature[c]	Age and lithostratigraphy[d]	TWT[a]	Compared[b] mbsf	Nearest feature[c]	Age and lithostratigraphy[d]	TWT[a]	Computed[b] mbsf	Nearest feature[c]	Age and lithostratigraphy[d]
1	200	180	175	late Pliocene hiatus within Unit I	200	180	174	Base late Miocene	200	180	160	Unit I and base late Pliocene	Base of unit cannot be traced to this site.[e]			
							213	middle Eocene Miocene boundary								
							230.5	Base IIA								
2	370	335	306	late Miocene hiatus	Base of unit cannot be traced to site				210	185	180	early-middle Miocene boundary	185[a]		184	early-middle Miocene boundary
			300													
			325	early-middle Miocene boundary												
			360	Base IIB												
3	630	590		middle Eocene	-				530	490		?Base not drilled	560	520		middle Eocene

[a] Depth of the base of the unit in two-way traveltime measured at the site.
[b] Depth computed from measurements on seismic profiles using the sonobuoy data of Whitmarsh et al. (1990).
[c] Where the computed depth does not coincide exactly with a significant stratigraphic boundary or hiatus, the depths of nearby features identified from drilling results are shown (see footnote d).
[d] Age of sediment (from de Kaenel and Villa, this volume) at depths shown is given, or nearest stratigraphically significant feature (see footnote c), plus relationship to lithostratigraphic units defined in the Leg 149 *Initial Reports* (Shipboard Scientific Party, 1994a-c).
[e] The base of seismic Unit 1 cannot be traced into the Site 900 area because the base of Unit 2 pinches out adjacent to Site 898 (Fig. 5C). Therefore the depth of the base of the combined Units 1 and 2 is shown at a depth of 185 m.

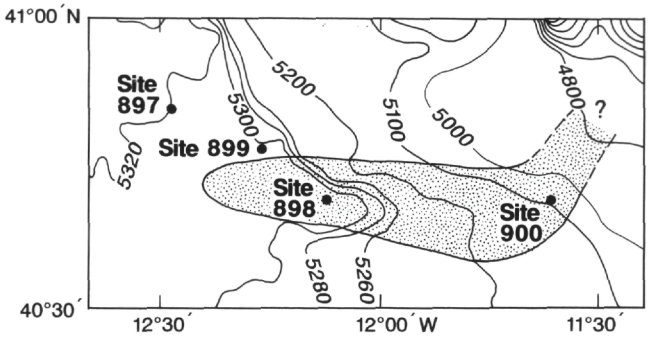

Figure 6. Map showing the distribution of the inclined reflection sequence in the vicinity of the Leg 149 sites. Light lines are the seismic coverage on which the map is based. Fine lines are bathymetric contours. Bold line outlines the area in which the inclined reflection sequence was observed. Modified from figure 4 of Shipboard Scientific Party (1994b).

cides with, and possibly caused, a major change in sedimentation. Sediments equivalent to Unit 3 are characterized by upward-darkening rhythms (5-15 cm thick) of carbonate-dominated turbidites and contourites with thin siliciclastic sand or silt bases and siliciclastic hemipelagic tops with sporadic nannofossil chalks. Silicoflagellates occur in these sediments but are absent in the lithologies equivalent to seismic Unit 2. Sediments equivalent to the latter unit consist of heavily bioturbated nannofossil claystones and oozes. The absence of silicoflagellates in sediments equivalent to seismic Unit 2 suggests that the upwelling of cooler bottom waters during seismic Unit 3 times was "shut down" at the same time as folding occurred; we do not have an explanation for this coincidence of events.

Unit 3

Unit 3: Description

The most characteristic feature of Unit 3 is the occurrence of westward-inclined reflections forming a sequence up to 230 ms thick between SP 3000 and 4000 on LG12 (Fig. 3C, back pocket; Fig. 5) and along almost the entire length of SO18 and SO20 (Fig. 3D, back pocket). The base of the inclined reflections defines the base of the unit. The only exception is a short length on SO20 at SP 200, where a separate narrow interval of inclined reflections occurs just below the top of Unit 4 (the separation is too small to be shown on Fig. 3D, back pocket, but is visible on the full-scale seismic line). Recognition of the base of Unit 3 in areas where there are no inclined reflections was achieved by tracing the reflection at the base of the inclined interval around the seismic grid. Unit 3 has a sheetlike geometry and ranges in thickness from 520 ms to the east of Site 900, diminishing to 200 ms west of Site 898, (LG12, SP 2600-2200, Fig. 3C, back pocket), and then thickening to 270 ms west of Site 897.

The interval of inclined reflections is laterally extensive on east-west lines (LG12, SO18, SO20, and SO22), thins west of Site 898, and disappears completely at about SP 2600 on LG12 (Fig. 3C, back pocket, Fig. 5). On lines LG06, SO16, and SO17 and to the east of Site 900 on LG12 the lateral equivalent to the inclined zone shows low- to moderate-amplitude reflections or is seismically almost transparent (Fig. 5). Figure 6 shows the inclined reflector sequence occupies an elongate zone extending some 60 km westward from Site 900, with a north-south width of about 15-20 km.

On north-south lines SO17, SO19, and SO21, Unit 3 shows moderate- to high-amplitude continuous reflections. Short lengths of oblique reflections occur on lines LG04, SO17, and SO19. Where the west-northwest–east-southeast–oriented line GP20 illustrated by Groupe Galice (1979) and shown here in Figure 7 intersects LG12 to the east of Site 900, it shows the oblique reflection pattern.

On LG12 between Sites 898 and 900 a zone of undulatory reflections occurs above the inclined interval with wavelengths of 1.5 to 2.0 km and amplitudes of 10-20 ms (Fig. 5). This pattern is just discernible on the larger scale *Sonne* lines, where slightly undulatory discontinuous reflections occur.

Discussion

At Sites 897, 898, and 900, drilling results show that Unit 3 is middle Eocene to early Miocene in age. Thinning (referred to above) is caused by erosion of the top of the unit over the fold structures at Site 897, but the decrease in thickness west of Site 898 on LG12 (Fig. 3D, back pocket) may be due both to distance from sediment sources on the continental slope and shelf and to an increase in interval velocity resulting from deeper burial.

The undulatory and inclined reflections described above are interpreted as related to structures formed by the migration of large-scale bed forms produced by contour currents. The height and wavelength of the undulatory reflections is comparable to bed forms observed along the western Iberia Abyssal Plain margin by Gardner and Kidd (1987) at depths greater than 4000 m. The waves show slight migration to the east, which is the opposite direction to flow directions observed along the foot of the margin by Gardner and Kidd, but this is not surprising, as both upcurrent and downcurrent migration of wave forms is common on sediment drifts (Faugéres and Stow, 1993).

The westward-inclined reflections characteristic of the base of Unit 3 are associated with short reflections dipping in the opposite direction (Fig. 5). The reflection pattern is superficially analogous to the arrangement of laminae in cross stratification produced when the migration of bed forms is accompanied by very low depositional rates or slight erosion on their upcurrent side. However, in this case the bed forms were probably migrating in an upcurrent, rather than downcurrent, direction. Thus, the westward-inclined reflections are analogous to cross stratification set boundaries and the short eastward-dipping reflections between them to cross strata. It must be stressed that the inclined reflections are not clinoforms indicating sediment progradation. The absence of the inclined reflections in other areas may be due to changes in rates of sedimentation and/or contour current strength.

The true dip of the inclined reflections is to the west, or within 10°-20° of this direction. This is consistent with Gardner and Kidd's (1987) observation that the orientation of sediment waves along the western Iberia Abyssal Plain Margin ranges between about 15° and 18° to the regional contours. In the Leg 149 area, the present-day regional contours trend approximately northwest-southeast or west northwest-east southeast (Fig. 6).

Unit 4

Unit 4: Description

The base of Unit 4 is defined as the downward change from strong continuous reflections to the very discontinuous reflections of Unit 5, which appears almost seismically transparent in comparison to the overlying unit. Unit 4 shows thinning and onlap toward basement highs, and its overall thickness steadily diminishes westward, from 600 ms between Sites 900 and 901 to 240-300 ms to the west of Sites 897 and 898. This unit consists largely of an interval dominated by moderate- to high-amplitude continuous reflections (Fig. 3, Figs. 5, 8). The lower part of the unit onlaps onto highs in the acoustic basement and so it is impossible to trace its base continuously along most seismic lines. Reflection convergence occurs toward the highs.

Discussion

The deepest borehole penetration into Unit 4 was achieved at Site 900, where upper Paleocene sediments rest on the acoustic basement, which consists of metagabbros. The change from strong continuous

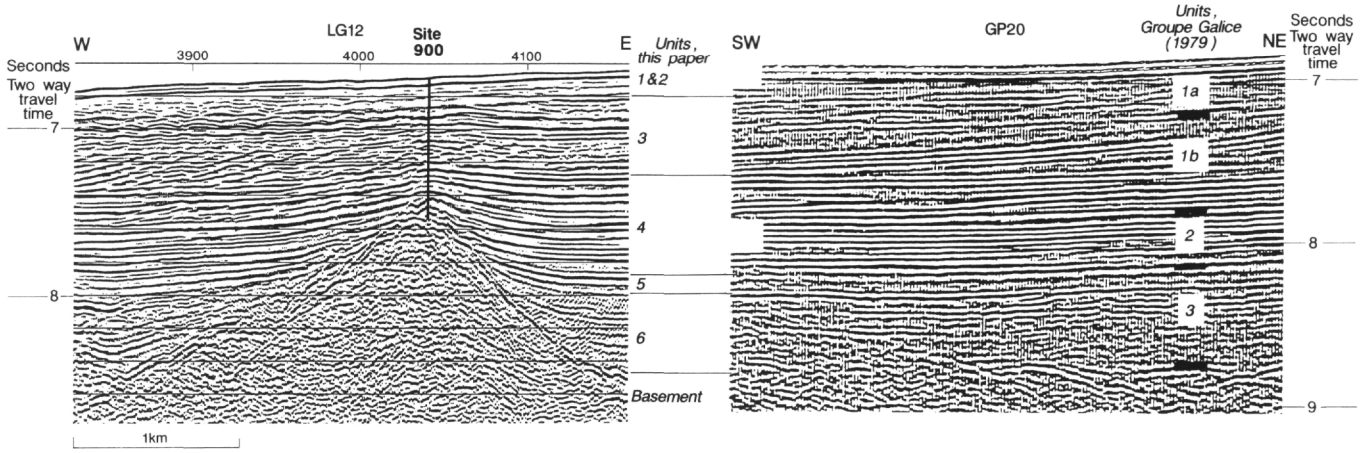

Figure 7. Part of migrated line LG12 and unmigrated line GP20 (from Groupe Galice, 1979, their fig. 9A, which does not show shotpoints or horizontal scale) to show how seismic units defined in this study correlate with those identified in the area of Site 398. Note the correlation between the interval of inclined reflectors on GP20 with the base of our Unit 3 and that between the base of our Unit 4 and Unit 2 of Groupe Galice. For reasons explained in the text, we consider that Groupe Galice failed to recognize their Unit 4 on this part of line GP20. We believe that the top of this unit occurs at 830 ms on the left side of the extract shown and correlates with the boundary between our Units 5 and 6.

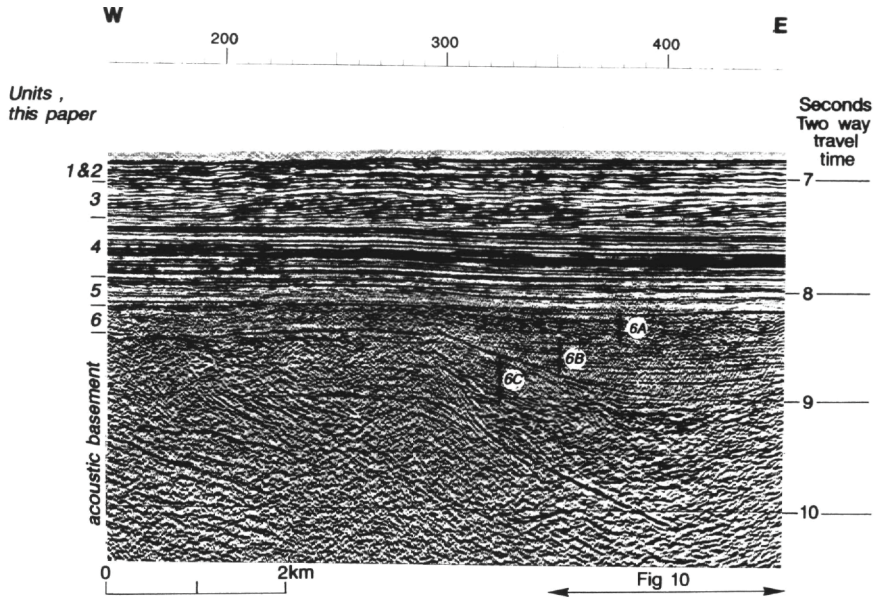

Figure 8. Part of migrated line SO18, showing all seismic units defined in this study, including three Subunits within Unit 6 (see Fig. 3D, back pocket, for interpretation). Note how between SP 250 and 400 Subunit 6C onlaps and downlaps onto acoustic basement.

to very discontinuous reflections across the boundary between Units 4 and 5 is very similar to that observed around Site 398 across the boundary between Units 2 and 3 of Groupe Galice (1979). This correlation is illustrated at the crossover of LG12 and GP 20 (Figs. 1, 7), where the base of Unit 4 of this study ties with the base of Unit 2 of Groupe Galice (1979). Drilling at Site 398 showed the boundary to be marked by a late Cenomanian-Turonian (and possibly Coniacian) age hiatus. Therefore, it is probable that Unit 4 in the Leg 149 area ranges in age from middle Eocene to Coniacian or late Santonian (Fig. 9).

Drilling at the Leg 149 sites showed that the top part of seismic Unit 4 consists of numerous upward-darkening units (10-30 cm thick) consisting of dominantly carbonate turbidites and siliciclastic hemipelagites, possibly reworked by contour currents. At Site 900, the siliciclastic sand content of the sequence is significantly higher, leading the Shipboard Scientific Party (1994c, p. 223) to suggest a possible lobe fringe setting on a submarine fan. On either side of Site 901, several mound features, between 150 and 400 ms high, are present within Unit 4 (Fig. 3C, back pocket). These are interpreted as sediment drifts formed between basement highs.

During the deposition of sediments equivalent to Unit 4, the basement highs west of Site 901 were completely buried. The lower part of Unit 4 onlaps the basement highs. The equivalent Unit 2 in the Group Galice (1979) study area shows some discordance and overstepping onto the underlying Unit 3, indicating tectonism related to Pyrenean movements; such features were not observed on the Iberia Abyssal Plain seismic profiles.

Units 5 and 6

Unit 5: Description

The base of Unit 5 is taken at a continuous high-amplitude reflection (in some areas by a pair of strong reflections on the *Lusigal* lines) or at the top of acoustic basement. Unit 5 is characterized by parallel,

low- to moderate-amplitude, low- to moderate-continuity reflections on the *Lusigal* lines, with slightly more continuity on the *Sonne* lines (Figs. 5, 8). However, on both groups of lines, the unit appears almost seismically transparent compared with the overlying high-amplitude continuous reflections of Unit 4. In the area west of Site 898, Unit 5 rests directly on acoustic basement or on a very discontinuous or rather chaotic reflection interval that may be equivalent to Unit 6. The unit onlaps basement highs. If thickness changes caused by draping over the highs are ignored, the unit shows an overall gradual thickening westward from ~ 60 ms adjacent to Site 900 to ~ 200 ms adjacent to Site 897 and in areas to the south of this site.

Unit 6: Description

Unit 6 drapes the irregular surface of the acoustic basement. It is recognized with confidence only east of a line through Sites 897 and 898. On the *Sonne* lines it shows moderate-amplitude semicontinuous to discontinuous reflections, but on the *Lusigal* lines higher amplitudes and continuity are usually displayed (compare Figs. 8, 5).

In the area between Sites 898 and 900, three Subunits can be recognized within Unit 6 on SO18, SO19, and SO20 and on a reprocessed version of LG12 (Krawczyk et al., this volume, their fig. 3). They are shown on Figure 3D, back pocket, and Figure 8. The descriptions below refer to appearance of the Subunits on SO18 and SO20 (Fig. 3D, back pocket; Figs. 5, 8).

Subunit 6A shows slightly undulatory, discontinuous, moderate- to high-amplitude reflections, capped by a moderate- to high-amplitude continuous reflector marking the boundary with Unit 5. This Subunit has a sheetlike geometry and is 200 ms thick; it dies out to the east at SP 180 on SO20, and to the west on SO18 it onlaps the basement ridge to the south of Site 898 (Fig. 3D, back pocket).

Subunit 6B shows parallel, low- to moderate-amplitude reflections that onlap onto the irregular topography of the acoustic basement. The Subunit onlaps Subunit 6C and is overstepped by Subunit 6A (Fig. 3D, back pocket; Fig. 8). To the east the boundary between Subunits 6A and B dies out at about SP 150 on SO20 (Fig. 3D, back pocket) where, in terms of seismic facies characteristics, it appears that Subunit 6A merges into Subunit 6B. Its thickness ranges from 0 to 600 ms.

Subunit 6C is a wedge-shaped reflection package, 0-250 ms thick, banked, to the west, against a steep slope in the acoustic basement between SP 200 and 400 on SO20 (Fig. 3D, back pocket; Fig. 8). It is about 10 km wide and almost transparent, but faint reflections downlap onto basement at the foot of slope and onlap onto the slope (Fig. 8).

Discussion

The tie between lines GP20 (Groupe Galice, 1979) and LG12 (Figs. 1, 7) shows that seismic Units 5 and 6 in the Leg 149 area are equivalent to Unit 3 of the earlier study. However, we question whether Groupe Galice correctly identified the base of Unit 3 on their figure 9A for the following reasons:

1. Apart from figure 9A of Group Galice (1979), their Unit 3 is shown in other extracts of seismic lines (e.g., their figures 8A, B, C; 9B, C; 15A) as being virtually transparent and not exhibiting significant reflection continuity. This seismic facies characteristic matches our Unit. 5.
2. The base of Group Galice's Unit 3 is characterized by a thin, strong reflection package on their figure 8.
3. It is not clear how Groupe Galice tied line GP20 (their figure 9A) to Site 398, as this line crosses the Vasco da Gama Seamount, against which all their units are shown to terminate at a fault boundary in their figure 9C, with their Unit 3 developing a sedimentary prism against the fault (but not showing reflection divergence toward the fault). The location of the extracts from seismic lines in the Groupe Galice paper is not clearly defined (neither is the horizontal scale given) but it appears that their figures 9C and 9A are contiguous as there is a perfect match between the depths of all the reflections shown at the northeast and southwest ends of the two extracts. Beneath the seismically virtually transparent prism a package of strong reflections occurs that is not identified as the base of their Unit 3, in contrast to the interpretation of another part of the line shown in their figure 9B, where the base of the unit is taken at the change from weak to strong reflections.

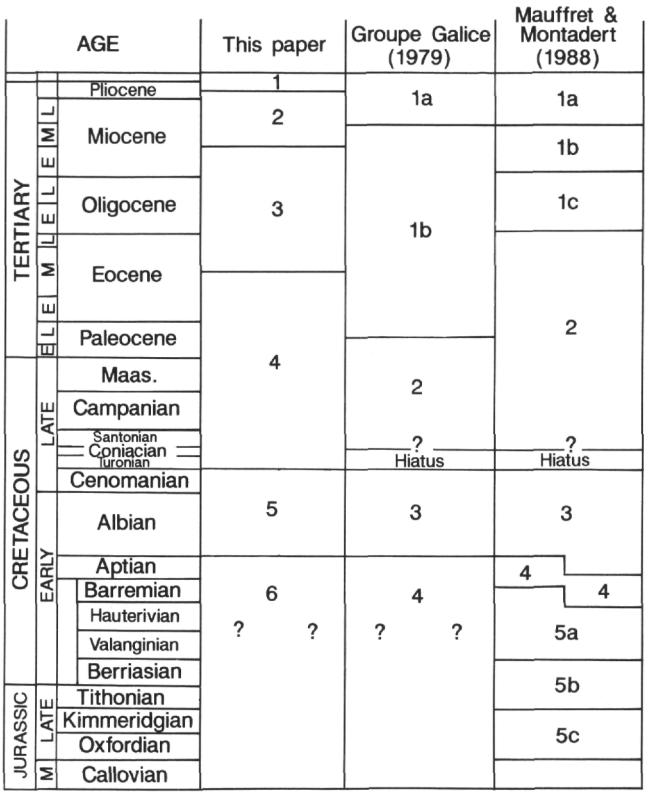

Figure 9. Comparison of the ages of seismic units identified in the Leg 149 area (this paper), at Site 898 (Groupe Galice, 1979), and in the Leg 103 area (Mauffret and Montadert, 1988).

In light of the above, we believe that the strong double reflection 130 ms below the base of Groupe Galice Unit 2 shown on line GP20 (on the right side of our Fig. 7) is the base of their Unit 3. This means that our Unit 5 equates to their Unit 3 as identified elsewhere in their study area, including the area of DSDP Site 398. Likewise, we equate our Unit 6 to Unit 4 of Groupe Galice. This interpretation is consistent with the strong similarities in reflection characteristics between the units defined in this study and those of Groupe Galice illustrated in Figure 10.

The correlation of our units with those of Groupe Galice as summarized in Figures 9 and 10 enables the former to be equated with the sequence drilled at Site 398. This indicates that Unit 5 is Albian to Cenomanian in age and that Unit 6 is Hauterivian to Aptian in age. If our Unit 6 is partly equivalent to Unit 5A of Mauffret and Montadert (1988), as suggested by comparing reflection characteristics as illustrated in Figure 10, then it may extend into the Valanginian.

At Site 398, the mid-middle Albian to Cenomanian interval consists of 236 m of marly nannofossil chalk to calcareous mudstone interbedded with dark gray to black claystone with minor siliciclastic sands. The remaining part of the Albian beneath this sequence comprises 218 m of dark gray to black laminated to homogeneous claystone. The low-amplitude/transparent nature of Unit 5 in the Leg 149 area suggests that similar sediments may occur here. The relatively stronger reflection characteristics of Unit 6 are consistent with the va-

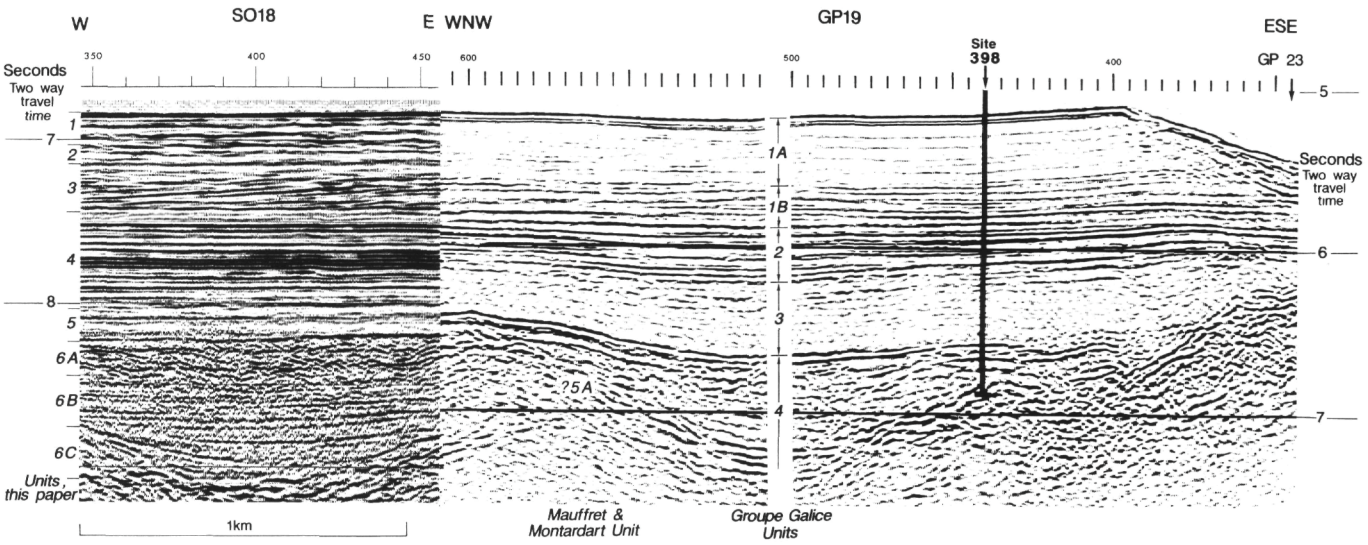

Figure 10. Comparison of parts of profile SO18 (see Fig. 3D, back pocket; Fig. 8) and GP19 at DSDP Site 398 (reproduced from figure 2A of Bouguigny and Wilm [1979] in which the horizontal scale is not indicated). Although these extracts are separated geographically by almost 100 km, there is a remarkable correlation between reflections within Unit 4 of this paper and Unit 2 of Groupe Galice. On line GP19, the strong double reflector at the base of the transparent interval is the boundary between Units 3 and 4 of Groupe Galice (1979). On Figure 7, this is shown to correlate with the base of our Unit 6, but this figure suggests, by comparing seismic facies, that it may equate to the top of our Unit 6 (i.e., the change from the transparent interval of Unit 5 to the stronger reflections of Unit 6). For reasons given in the text, we consider the correlation shown here more likely.

riety of lithologies found over the equivalent interval at Site 398. Here, the Aptian-Barremian sediments include black to dark dray and olive green mudstones and claystones with interbedded mud and limestone pebble debris flows and siliciclastic turbidites. The Hauterivian consists of radiolarian-rich nannofossil limestones interbedded with dark mudstones with some thin siliciclastic turbidites (Sibuet, Ryan, et al., 1979).

The wedge shape of Subunit 6C and the faint internal reflection pattern (Fig. 3D, back pocket; Fig. 8) suggest eastward progradation of a submarine fan or talus deposit.

Summary

The principal features of the seismic units beneath the Iberia Abyssal Plain are summarized in Table 2, and the relationships betweeen them illustrated in Figure 11.

TECTONIC HISTORY

Seismic and borehole data usually enable three approaches understanding the tectonic history of a given area. The first is a qualitative assessment of seismic sections to determine whether any synrift reflection packages can be identified so that, once the equivalent sediments are sampled for biostratigraphic analysis, the timing of rifting can be established. The other two approaches are quantitative. One uses borehole data to undertake a backstripping analysis to compute basement subsidence: in the Leg 149 area, the incomplete stratigraphic record obtained over basement highs precludes this approach. The other quantitative method uses digitized seismic profiles to estimate total tectonic subsidence along the profiles, from which extension factors (β) and crustal thickness are determined.

Tectonostratigraphic Units

Prosser (1993) proposed that distinct stages of rift evolution can be recognized, each with distinctive expressions on seismic profiles. She recognized four phases of development in rift basins: rift initiation, rift climax, immediate postrift, and late postrift. Her conclusions were based largely on studies of basins developing beneath relatively shallow seas, but included the Armorican Margin on the north side of the Bay of Biscay. She showed that footwall crests and hanging walls may be eroded in subaerial and shallow-marine realms and so contribute sediments to the deeper parts of the basin. In such basins, tectonic movements play a crucial role in creating—or destroying—accommodation space in which sediments may accumulate. However, in rift basins that remain in the submarine realm throughout their history, the crests of tilted fault blocks will not be subjected to subaerial erosion and so will not contribute significant amounts of sediment to adjacent basins, except by mass wasting processes. This means that sediment transport into the basin will be dominated by gravity-driven processes and pelagic/hemipelagic sedimentation. Little sediment will be derived locally by marine or subaerial erosion, but there may be gravity-driven resedimentation from both the hanging wall and footwall as rifting develops and the gradient of the slopes increases.

Rotation of fault blocks during rifting results in three features that may be resolvable on seismic reflection profiles. First, synrift reflection packages should show thickening toward footwalls, and, second, rotation may also result in later packages onlapping earlier ones toward the hanging wall. Some erosional truncation might occur between packages if sediments were transported toward the footwall by slumping or debris flows. Third, the crests of tilted fault blocks will show significant erosional features if they are uplifted above sea level: no such features are visible on seismic profiles in the Leg 149 area. Even the most elevated crest in the study area, the tilted fault block beneath Site 901 (Fig. 3C, back pocket), which is capped by Tithonian clays and minor sandstones, shows no erosional truncation on a reprocessed version of part of LG12 shown as Figure 9 in Krawczyk et al. (this volume). This suggests that the rift system from Site 901 westward developed entirely in a submarine environment.

No seismic lines in the Leg 149 area show reflection divergence into steep slopes on top of the acoustic basement that are candidate fault scarps. The topography of the acoustic basement is draped by Units 6, 5, and 4, all of which show onlap and thinning toward basement slopes. Even adjacent to the extremely large fault scarp immediately to the west of Site 901 on line LG12 (Fig. 5C; Fig. 1 of Beslier, this volume; fig. 3 of Krawczyk et al., this volume) there is no clear reflection divergence. The only possible exception occurs on

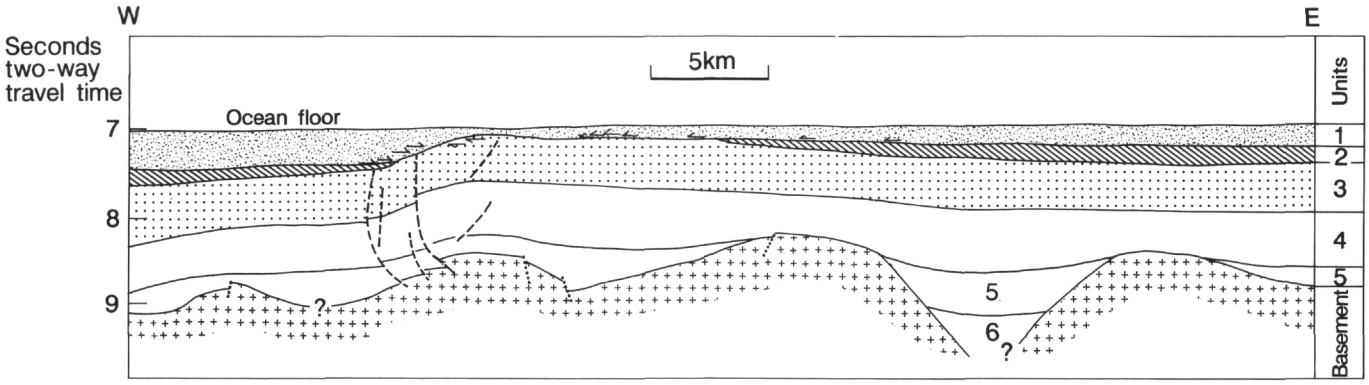

Figure 11. Reinterpretation of figure 3 from Masson et al. (1994) showing fold structure interpreted on part of profile LG14 (see Fig. 3, back pocket, for location). This section displays the following key relationships between the seismic units described in this paper: (1) onlap and erosional truncation of Unit 1 (late Pliocene to Holocene) and older units over fold; (2) thinning of Unit 2 (middle Miocene to late Pliocene) toward the fold crest (the main phase of deformation occurred at the early/middle Miocene boundary); and (3) Units 5 (Albian to Cenomanian) and 6 (Hauterivian/possible Valanginian, to Aptian) passively infill fault-related topography in the acoustic basement and are not synrift units.

Table 2. Summary of the principal features of seismic units identified in the Leg 149 area.

Unit	Age of base	Thickness (ms TWT)	Geometry, onlap, etc.	Probable lithology	Additional comments
1	late Pliocene	100–200	Sheet, but thickens significantly on west sides of folds. Base onlaps/truncates Unit 2 and erodes into Unit 3 in crestal locations	Siliciclastic turbidites and pelagic nannofossil oozes	Units 1 and 2 cannot be distinguished east of Site 898, where influence of contour currents is indicated by undulatory reflections
2	middle Miocene	0–460	Wedge, thinning, and onlapping toward crests of folds, and absent over crests	As above with bioturbated hemipelagites and pelagic nannofossil rich sediments at base	
3	middle Eocene	150–520	Lower boundary defined by base of inclined reflection interval and its correlative reflector. Sheet-like geometry with gradual westward thinning.	Carbonate turbidites (with minor siliciclastics at base) siliciclastic hemipelagites, and contourites	Inclined interval of reflection marks base of unit between Sites 898 and 900 and indicates influence of contour currents
4	?Santonian/Coniacian (by comparison with Site 398)	240–600	Sheet with high-amplitude continuous reflections but basal part onlaps highs in acoustic basement	As above, but becomes more siliciclastic sand rich in the lower part of the Eocene at Site 900	Oldest equivalent sediment drilled at Site 900 is Paleocene in age
5	?Albian	0–600	Moderate- to weak-amplitude reflections. Three subunits recognized; wedge-shaped lowermost subunit suggests progradational depositional system	Comparison with Site 898 suggests older, siliciclastic turbidites and debris flows with carbonate clasts	

the reprocessed version of LG12 (Krawczyk et al., this volume, their figs. 3, 12) between SP 4300 and 4400 at about 8.5 ms TWT, where there is some indication of a reflection package thickening into a low-angle fault plane dipping westward. Beslier et al. (1995) also interpreted this part of the profile as a synrift interval, but we believe it is more likely the result of drape and compaction over an earlier fault-induced topography.

The absence of convincing examples of synrift reflection geometries may be due to very low sedimentation rates during the rift climax in deep-sea settings. The creation of a series of long hanging-wall slopes and footwall scarps will mean that turbidity and debris flows will be ponded back in more landward basins. Therefore, only the more dilute portions of turbidity currents are likely to flow through the maze of ridges and hollows created by rifting and deposit sediment in the deeper parts of deep-sea rift zones. During the rift-climax phase, sedimentation in such areas is most likely dominated by pelagic and hemipelagic settling. In such a situation, rifting and contemporaneous deposition would have to continue for several million years to produce seismically resolvable reflection packages showing divergence.

Our scrutiny of published lines from the Leg 103 area (Mauffret and Montadert, 1988; Winterer et al., 1988) and around Site 389 (Groupe Galice, 1979) revealed no convincing reflection divergence into faults indicating significant deposition during rifting. Therefore, we suggest that these earlier studies did not correctly identify the seismostratigraphic expression of the rifting episode. We agree with the view of Prosser (1993, p. 51) that ignoring the importance of infilling remnant topography in the creation of overall wedge-shaped geometries and the possibility of divergent reflector configurations induced by compaction can lead to overestimations in the duration of active faulting. The extent of such an overestimate in the Galicia Margin area is illustrated in Figure 12.

In the light of the discussion above, we conclude that rifting occurred prior to the deposition of sediments equivalent to our Unit 6, which is Hauterivian (and possibly Valanginian) to Aptian in age (Figs. 9, 10). The faint progradational reflection geometry in Subunit 6C, situated immediately over a possible fault scarp on line SO18 (Fig. 8), may be an immediate postrift feature in terms of Prosser's (1993) rift phases.

At Site 398, ill-defined curved reflection patterns in Unit 4 of Groupe Galice (1979) could indicate drape and compaction over fault-induced topography (Fig. 10). This suggests that this unit is probably postrift in origin, in which case the rifting must predate the Hauterivian age obtained from the oldest sediments drilled at Site 398 and postdate the Tithonian sediments drilled at Site 901. The timing of rifting can be better constrained in the deep Galicia Margin ar-

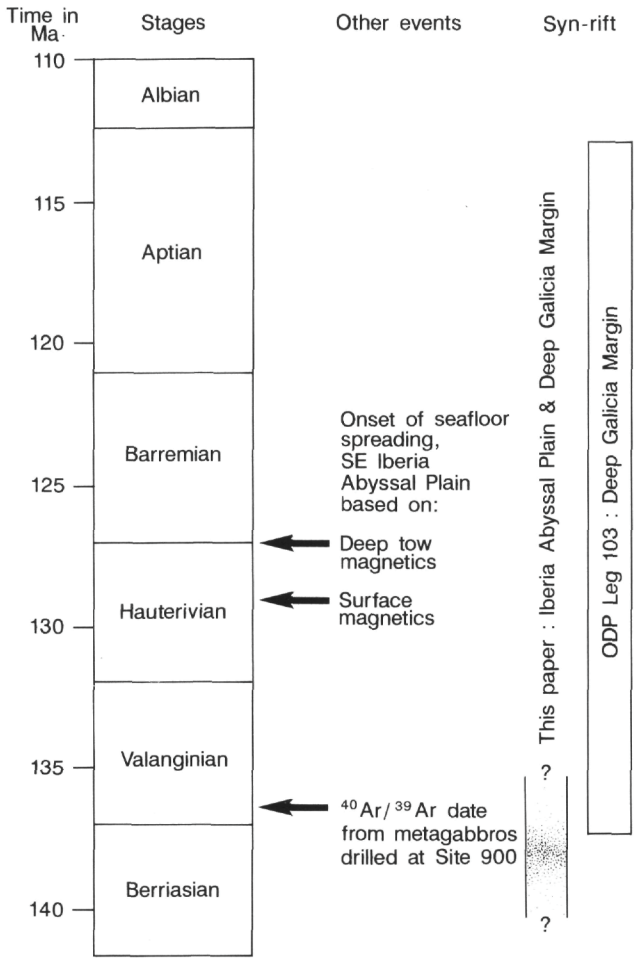

Figure 12. Key events in the geological history of the eastern margin of the Iberia Abyssal Plain. The short duration of rifting proposed in this paper is contrasted with the prolonged synrift episode identified by Boillot and Winterer (1988). The age of the onset of seafloor spreading is based on modeling surface and deep-tow magnetic data from the southeastern part of the Iberia Abyssal Plain (Whitmarsh and Miles, 1995; Whitmarsh et al., this volume). The $^{40}Ar/^{39}Ar$ date for metagabbros drilled at Site 900 is a closure age for plagioclase subjected to low-temperature shear deformation (Féraud et al., this volume). The Gradstein et al. (1994) time scale is used in this figure.

ea. Here, Tithonian-Berriasian shelf carbonates drilled during Leg 103 are clearly prerift in origin and are identified as such on published seismic lines (Mauffret and Montadert, 1988; Winterer et al., 1988). However, according to our reinterpretation of the published lines, the reflection package equivalent to the upper Valanginian to Aptian siliciclastic sediments above the carbonate interval is postrift, not synrift, in origin. This suggests that rifting occurred during latest Berriasian and earliest Valanginian times in the Leg 103 area. Given the suggested correlation of seismic units beneath the Iberia Abyssal Plain with those beneath the deep Galicia Margin (Figs. 9, 10), rifting probably occurred between the late Berriasian and early Valanginian in both areas. This constrains the age of rifting to between about 134 and 140 Ma (using the Mesozoic time scale of Gradstein et al., 1994). The $^{40}Ar/^{39}Ar$ age of 136.4 ± 0.3 Ma (early Valanginian) related to late low-temperature shear deformation during the last stages of continental rifting (Féraud et al., this volume) is consistent with the timing of rifting suggested in this paper.

Figure 12 summarizes the ages of key events at the eastern margin of the Iberia Abyssal Plain. It suggests that rifting occurred over a relatively short period of time (~5 m.y.) during the late Berriasian and early Valanginian and was followed about 6-8 m.y. later by the onset of seafloor spreading beneath the southeastern part of the Iberia Abyssal Plain. This time gap between the end of rifting could be explained by our conclusion about the age and duration of rifting in this area being incorrect. However, off the Galicia Margin, the commencement of seafloor spreading should have been later if ocean opening propagated northward, but here the age of rifting is much better constrained to be late Berriasian-early Valanginian by correlating seismic and drilling data. The time gap between the cessation of rifting and the onset of seafloor spreading in both areas suggests either that there was a temporary suspension of plate movement (which is unlikely) or that extension was transferred to another location that could have been situated on the Grand Banks conjugate margin.

The conclusion that our Unit 6 is Aptian to possible Valanginian in age only increases the difficulty of interpreting the setting of the Aptian debris flows and rock-fall breccias encountered on the crest of basement highs at Sites 897 and 899. These occurrences are about 1 km higher than Unit 6. Yet there is no evidence for the basement ridge at Site 897 being tectonically uplifted, or rising diapirically, during the deposition of Units 1-4. Elsewhere in areas also presumed underlain by serpentinite ridges (i.e., the area around Site 898), there is no sign (such as significant reflection thinning and rotation toward areas of uplift) of Units 5 and 6 being affected by localized uplifts. This conclusion is at odds with comments made by Comas et al. (this volume) and Gibson, Morgan, and Milliken (this volume) to the effect that the basement topography that existed at the time of formation of the Aptian olistostromes incorporating mantle material drilled at Sites 897 and 899 differed significantly from that observed today. In particular, we see no evidence that Units 5 and 6 were affected by latest Cretaceous postrift tectonics as suggested by Comas et al. (this volume) to account for the occurrence of olistostromes on basement highs. Debris-flow deposits, such as those occurring in lithostratigraphic Unit IV at Site 897 (Shipboard Scientific Party, 1994a) and Subunit IVB at Site 899 (Shipboard Scientific Party, 1994c) require only gentle (<1°) slopes for their formation (Stow, 1994) and so could have been generated on the basement topography observed today. However, the rock-fall origin (Gibson, Morgan, and Milliken, this volume) for the serpentinite breccias of Subunit IVA at Site 899 implies the existence of nearby slopes inclined at 15° or more (Stow, 1994). As this site was surveyed only by low-resolution single-channel *JOIDES Resolution* data, its topographic setting is not well constrained.

Subsidence of Individual Sites

The subsidence experienced by any point on a rifted continental margin includes thermal subsidence with a time constant of approximately 63 Ma (Parsons and Sclater, 1977), which begins at about the end of the rifting process, and subsidence in response to sediment loading, which depends on the sedimentation history of the margin. To begin to understand the tectonic history of the Iberia Abyssal Plain Margin, we intended to investigate the subsidence of the three Leg 149 sites that had the greatest penetration of the sedimentary column (Sites 897, 899, and 900; Sawyer, Whitmarsh, Klaus, et al., 1994). At these three sites we had hoped to obtain the information required to conduct a backstripping analysis (paleodepth estimates and a knowledge of the lithology, porosity, and biostratigraphic ages of the sediments). In principle this should have enabled us to compute the basement subsidence by taking account of sediment loading, water depth at the time of deposition, and sea-level changes (Steckler and Watts, 1978). A similar approach was used successfully at the Galicia Bank Margin by Moullade et al. (1988). However, given the above time constant, in theory most subsidence occurs within the first 50 Ma after rifting ceases. The latest onset of thermal subsidence along the Leg 149 transect was at about 130 Ma, which is our best estimate of the beginning of seafloor spreading there (see Whitmarsh et

al., this volume). Thus, to constrain the subsidence, we need paleodepth estimates from sediments laid down in the Aptian to latest Cretaceous age interval. Unfortunately, almost no in situ sediments of this age were recovered from the Leg 149 sites. Consequently, only the most limited estimates have been made of paleodepth (Table 3). We are almost sure that the Tithonian sediments at Site 901 were deposited in neritic depths (approximately 200 m) but all other cores containing benthic foraminifers that were used to estimate paleodepth are Paleocene or younger in age and indicate depths in excess of 4200 m (Collins, Scott, and Zhang, this volume; Collins, Kuhnt, and Scott, this volume; Kuhnt and Collins, this volume). While these depths are broadly consistent with the onset of subsidence about 130 Ma, they give virtually no constraints on the history of the critical first 50 Ma of subsidence.

Table 3. Summary of paleodepth estimates from Leg 149 Sites 897-901.*

Site	Cores	Depth (mbsf)	Water depth (m)	Paleodepth (m)	Biostratigraphic age
897C	60 to 61	630	5320	>4200	late Paleocene–early Eocene
897D	1 to 3	610	5320	4000–4200	middle Eocene
897D	3 to 4	630	5320	>4000–4500	early Eocene
897D	5	640	5320	>4000–4500	Paleocene
897D	6 to 10	670	5320	(<200)**	Aptian
898A	1 to 18	80	5280	4500–5820	Pliocene/Pleistocene
898A	18 to 27	205	5280	3500–5280	Miocene
899B	13, 14	350	5291	>4000–4500	middle Eocene
900A	1 to 13	55	5036	4500–5036	Pliocene/Pleistocene
900A	14 to 34	215	5036	3500–5036	Miocene
900A	70 to 76	685	5036	>4200	Eocene
900A	78	735	5036	>4200	Paleocene
910A	2 to 7	182	4718	<200	Tithonian

Notes: *from Collins et al., this volume; Kuhnt and Collins, this volume; **these samples are from a debris flow and hence are almost certainly allochthonous.

Total Tectonic Subsidence and Crustal Extension

Method

We used the bathymetry and basement depth along the digitized seismic profiles to estimate total tectonic subsidence, the sediment-unloaded depth to basement (Sawyer, 1985). We included the effects of sediment compaction and local isostatic compensation in our calculation. We computed the average sediment density (ρ_s) between the seafloor and basement assuming an exponential decrease in porosity (ϕ) with depth z, sediment grain density (ρ_{sg}) of 2650 kg/m^3, porosity at the seafloor (ϕ_0) of 0.55, an exponential porosity decrement c of 4.5 $\times$ 10^{-4}/m, and sediment thickness (S). The result is not very sensitive to the sediment compaction parameters:

$$\phi = \phi_0 e^{-cz}, \quad (1)$$

$$\rho_s = \phi\rho_w + (1 - \phi)\rho_{sg}, \text{ and} \quad (2)$$

$$\rho_s = \frac{1}{S}\int_0^{\infty} \rho_s \, dz. \quad (3)$$

Using this sediment density model, water depth (W), water density (ρ_w) = 1030 kg/m^3, and mantle density (ρ_m) = 3300 kg/m^3, we computed TTS (Y) on a point-by-point basis along the profiles assuming local isostatic compensation (Steckler and Watts, 1978):

$$Y = S\left[1 - \frac{\rho s - \rho w}{\rho m - \rho w}\right] + W \quad (4)$$

To eliminate the roughness of the TTS owing to local basement topography (Sawyer, 1986), the TTS was smoothed for subsequent calculations using a 50-km running-average filter. Extension during rifting may be estimated using TTS if one assumes isostasy and that the current basement surface was at sea level prior to rifting. In this case, the present depth to basement, after sediment unloading, is the total amount of tectonic subsidence of the crust during and since rifting. Within extended continental crust, the TTS is related to the crustal extension (β) (Fig. 13) (Le Pichon and Sibuet, 1981; Dunbar, 1988) by

$$Y = C\left(1 - \frac{1}{\beta}\right), \quad (5)$$

where

$$C = 3.6 + 4.2(1 - e^{-t/\tau}) \text{ km}. \quad (6)$$

The constant of proportionality (C) is a function of the age of continental breakup (t). The thermal time constant (τ) is 62.8 m.y. (Sclater et al., 1980). For old rifted margins, with ages greater than one thermal time constant, the relationship between TTS and (β is relatively insensitive to the duration of the breakup process, variations in the initial crustal thickness, or whether extension is accomplished by stretching or dike intrusion (Dunbar and Sawyer, 1989). We have estimated β in this study for rifting at 135 Ma (Fig. 13). Modeling magnetic anomaly data from the western part of the study area indicates that seafloor spreading commenced at 129-127 Ma (Fig. 12). As discussed earlier, we believe rifting occurred between 134 and 140 Ma.

Given the variation of β across a margin, one can estimate the variation in crustal thickness. This estimate is valid to the extent that the original crustal thickness was constant in the rifted region and can be inferred from the present crustal thickness in the adjacent unextended region and to the extent that no new material was added to the crust by magmatic intrusion or underplating. The estimate of extended crustal thickness is the original crust thickness divided by β. In this study we estimated crustal thickness using values of β derived for a rifting age of 135 Ma. We estimated the depth of the crust/mantle boundary by adding the estimated crustal thickness to the smoothed (50-km running average) basement depth.

Our TTS method estimations of β and crustal thickness do not include the affects of dike intrusion. Dike intrusion during rifting should be accounted for in the estimated β in that it is just one of several possible mechanisms of crustal extension. Dike intrusion probably increases the density of the extended continental crust, which will cause the basement to subside more than predicted for a given β. Thus, it may lead to a small overestimate of β. In addition, the intrusion of new material into the extended continental crust will make the actual crust, as measured using seismic refraction, thicker than we estimate using the TTS method.

The TTS estimation of crustal thickness does not include the affects of serpentinization of the upper mantle. Serpentinization of a layer of upper mantle, because it involves a density reduction, would cause the TTS to be less than it would be otherwise. This would work its way through the calculations to reduce the estimated β and increase the estimated crustal thickness. If the serpentinized layer was correctly identified using seismic refraction and not included as part of the crust, then the TTS crustal thickness estimate would be greater than the actual crustal thickness.

Results

The smoothed TTS for the western (seaward) end of profile *Lusigal* 12 (Fig. 14; distance 0-140 km) is between 6.0 and 6.3 km. This is consistent with the subsidence of normal oceanic crust formed $\geq$100 Ma or continental crust thinned by β of between 5 and 7 at 135 Ma. There is an inflection at about 140 km with decreasing TTS and β to the east.

This is most simply interpreted as extended continental crust with decreasing extension to the east. The Moho depths predicted using the TTS data are somewhat deeper than those observed using seismic

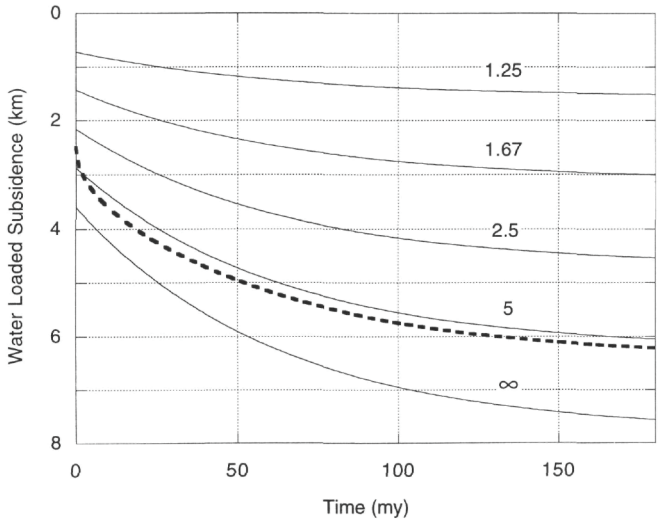

Figure 13. Predicted TTS vs. time since rifting or ocean crust creation for extended continental crust (curves with β labelled) and normal oceanic crust (dashed line; Sclater et al., 1980). Note that for the rifting age appropriate to this study, 135 Ma, the subsidence of normal oceanic crust is about the same as that of continental crust extended by β = 5.7.

refraction (Whitmarsh et al., 1990a). The TTS estimates should be compared to the depth of the base of the crust (Fig. 14; squares for L2 and L3 and circle for L1). The material below that boundary for lines L2 and L3 is interpreted to be serpentinized peridotite formed by hydration of the upper mantle. For the purposes of this analysis, this serpentine is part of the upper mantle, rather than the crust. The TTS-predicted Moho is about 2-4 km deeper than the seismic refraction base of the crust. We see three possibilities for explaining this discrepancy. First, it may indicate that the prerift crustal thickness we chose, 40 km, was too large. Using 30 km would remove about one-half of the discrepancy. Second, as discussed above, the process of serpentinization of the upper mantle will bias the TTS estimate of crustal thickness upward and therefore Moho depth downward. The third possibility is that we are incorrectly interpreting this crust as extended continental crust. The method used to estimate β and crust thickness is based on that assumption. If this were not extended continental crust, then the top and bottom panels are meaningless.

The remaining profiles (Figs. 14B-14L) show TTS consistent with β of between 5 and 7 with sporadic excursions as high as 9 and as low as 4. These may be interpreted as the same as the west end of profile *Lusigal* 12 (Fig. 14). That is, they are consistent with the subsidence of normal oceanic crust formed ≥100 Ma or continental crust thinned by the indicated β with rifting occurring at 135 Ma. Using these data alone, there is no way to select from these interpretations.

Summary

The second part of this study documents the following key points concerning the tectonic history of the Iberia Abyssal Plain.

1. *Rifting.* No direct evidence for the accumulation of synrift sediments was observed on seismic sections. Therefore, the main rifting event must predate our Unit 6, which is Aptian to Hauterivian (and possibly Valanginian in age), and postdate Tithonian siliciclastics drilled at Site 901 and Tithonian-Berriasian carbonates penetrated in the Leg 103 area. Rifting probably occurred between 140 and 134 Ma.
2. *Basement topography.* There is no evidence to suggest that basement topography established during rifting was modified by later deformation.
3. *Total tectonic subsidence* calculated along the interpreted seismic profiles indicates continental crust thinned by β of between 5 and 7 at 135 Ma. At the western end of the study area, TTS of about 6 km is consistent with the subsidence of normal oceanic crust formed ≥100 Ma.

ACKNOWLEDGMENTS

We thank Gilbert Boillot for providing copies of the *Lusigal* seismic lines and Karl Hinz for copies of the *Sonne* lines. The constructive comments of Doug Masson, Sarah Prosser, and an anonymous reviewer are gratefully acknowledged. The preparation of this paper was aided greatly by Denise Swann (word processing) and Andrew Lloyd and John Taylor (cartography). We thank the Leg 149 Shipboard Scientific Party and the ship and drilling crews for enabling lithostratigraphic and biostratigraphic data to be collected to "calibrate" the seismic interpretations presented in the paper.

REFERENCES

Beslier, M.O., Bitri, A., and Boillot, G., 1995. Structure de la transition continent-océan d'une marge passive: sismique réflexion multitrace dans la Plaine Abyssale Ibérique (Portugal). *C. R. Acad. Sci. Ser. 2,* 320:969-976.

Boillot, G., and Winterer, E.L., 1988. Drilling on the Galicia Margin: retrospect and prospect. *In* Boillot, G., Winterer, E.L., et al., *Proc. ODP, Sci. Results,* 103: College Station, TX (Ocean Drilling Program), 809-828.

Bouguigny, R., and Wilm, C., 1979. Tentative calibration of Site 398 and special processing of parts of Lines GP-19 and GP-23. *In* Sibuet, J.-C, Ryan, W.B.F., et al, *Init. Repts. DSDP,* 47 (Pt. 2): Washington (U.S. Govt. Printing Office), 623-629.

Dunbar, J.A., 1988. Kinematics and dynamics of continental breakup [Ph.D. dissert.]. Univ, of Texas, Austin.

Dunbar, J.A., and Sawyer, D.S., 1989. Effects of continental heterogeneity on the distribution of extension and shape of rifted continental margins. *Tectonics,* 8:1059-1078.

Faugères, J.C., and Stow, A.V., 1993. Bottom-current-controlled sedimentation: a synthesis of the contourite problem. *Sediment. Geol,* 82:287-297.

Gardner, J.V., and Kidd, R.B., 1987. Sedimentary processes on the northwestern Iberian continental margin viewed by long-range side-scan sonar and seismic data. *J. Sediment. Petrol,* 57:397-407.

Gradstein, F.M., Agterberg, F.P., Ogg, J.G., Hardenbol, J., van Veen, P., Thierry, J., and Huang, Z., 1994. A Mesozoic time scale. *J. Geophys. Res.,* 99:24051-24074.

Groupe Galice, 1979. The continental margin off Galicia and Portugal: acoustical stratigraphy, dredge stratigraphy, and structural evolution. *In* Sibuet, J.-C., Ryan, W.B.F., et al., *Init. Repts. DSDP,* 47 (Pt. 2): Washington (U.S. Govt. Printing Office), 633-662.

Le Pichon, X., and Sibuet, J.C., 1981. Passive margins: a model of formation. *J. Geophys. Res.,* 86:3708-3720.

Masson, D.G., Cartwright, J.A., Pinheiro, L.M., Whitmarsh, R.B., Beslier, M.-O., and Roeser, H., 1994. Localized deformation at the ocean-continent transition in the NE Atlantic. *J. Geol. Soc. London,* 151:603-613.

Mauffret, A., and Montadert, L., 1988. Seismic stratigraphy off Galicia. *In* Boillot, G., Winterer, E.L., et al., *Proc. ODP, Sci. Results,* 103: College Station, TX (Ocean Drilling Program), 13-30.

Moullade, M., Brunet, M.-F., and Boillot, G., 1988. Subsidence and deepening of the Galicia Margin: the paleoenvironmental control. *In* Boillot, G., Winterer, E.L., et al., *Proc. ODP, Sci. Results,* 103: College Station, TX (Ocean Drilling Program), 733-740.

Parsons, B., and Sclater, J.G., 1977. An analysis of the variation of ocean floor bathymetry and heat flow with age. *J. Geophys. Res.,* 82:803-829.

Prosser, S., 1993. Rift-related linked depositional systems and their seismic expression. *In* Williams, G.D., and Dobb, A. (Eds.), *Tectonics and Seismic Stratigraphy.* Geol. Soc. Spec. Publ. London, 71:35-66.

Sawyer, D.S., 1985. Total tectonic subsidence: a parameter for distinguishing crust types at the U.S. Atlantic continental margin. *J. Geophys. Res.,* 90:7751-7769.

———, 1986. Effects of basement topography on subsidence history analysis. *Earth Planet. Sci. Lett.,* 78:427-434.

Sawyer, D.S., Whitmarsh, R.B., Klaus, A., et al., 1994. *Proc. ODP, Init. Repts.,* 149: College Station, TX (Ocean Drilling Program).

Sclater, J.G., Jaupart, C, and Galson, D., 1980. The heat flow through oceanic and continental crust and the heat loss of the Earth. *Rev. Geophys. Space Phys.,* 18:269-311.

Shipboard Scientific Party, 1994a. Site 897. *In* Sawyer, D.S., Whitmarsh, R.B., Klaus, A., et al., *Proc. ODP, Init. Repts.,* 149: College Station, TX (Ocean Drilling Program), 41-113.

———, 1994b. Site 898. *In* Sawyer, D.S., Whitmarsh, R.B., Klaus, A., et al., *Proc. ODP, Init. Repts.,* 149: College Station, TX (Ocean Drilling Program), 115-146.

———, 1994c. Site 899. *In* Sawyer, D.S., Whitmarsh, R.B., Klaus, A., et al., *Proc. ODP, Init. Repts.,* 149: College Station, TX (Ocean Drilling Program), 147-209.

Sibuet, J.-C., Ryan, W.B.F., et al., 1979. *Init. Repts. DSDP,* 47 (Pt. 2): Washington (U.S. Govt. Printing Office).

Steckler, M.S., and Watts, A.B., 1978. Subsidence of Atlantic-type continental margin off New York. *Earth Planet. Sci. Lett.,* 41:1-13.

Stow, D.A.V., 1994. Deep sea processes of sediment transport and deposition. *In* Pye, K. (Ed.), *Sediment Transport and Depositional Processes:* Oxford (Blackwell Scientific), 257-291.

Whitmarsh, R.B., and Miles, P.R., 1995. Models of the development of the West Iberia rifted continental margin at 40°30'N deduced from surface and deep-tow magnetic anomalies. *J. Geophys. Res.,* 100:3789-3806.

Whitmarsh, R.B., Miles, P.R., and Mauffret, A., 1990a. The ocean-continent boundary off the western continental margin of Iberia, I. Crustal structure at 40°30'N. *Geophys. J. Int.,* 103:509-531.

Whitmarsh, R.B., Miles, P.R., and Pinheiro, L.M., 1990b. The seismic velocity structure of some NE Atlantic continental rise sediments: a lithification index? *Geophys. J. Int.,* 101:367-378.

Wilson, R.C.L., Hiscott, R.N., Willis, M.G., and Gradstein, F.M., 1989. The Lusitanian Basin of west-central Portugal: Mesozoic and Tertiary tectonic, stratigraphic and subsidence history. *In* Tankard, A.J., and Balkwill, H.R. (Eds.), *Extensional Tectonics and Stratigraphy of the North Atlantic Margins.* AAPG Mem., 46:341-361.

Winterer, E.L., Gee, J.S., and Van Waasbergen, R.J., 1988. The source area for Lower Cretaceous clastic sediments of the Galicia Margin: geology and tectonic and erosional history. *In* Boillot, G., Winterer, E.L., et al., *Proc. ODP, Sci. Results,* 103: College Station, TX (Ocean Drilling Program), 697-732.

Date of initial receipt: 5 December 1994
Date of acceptance: 24 August 1995
Ms 149SR-245

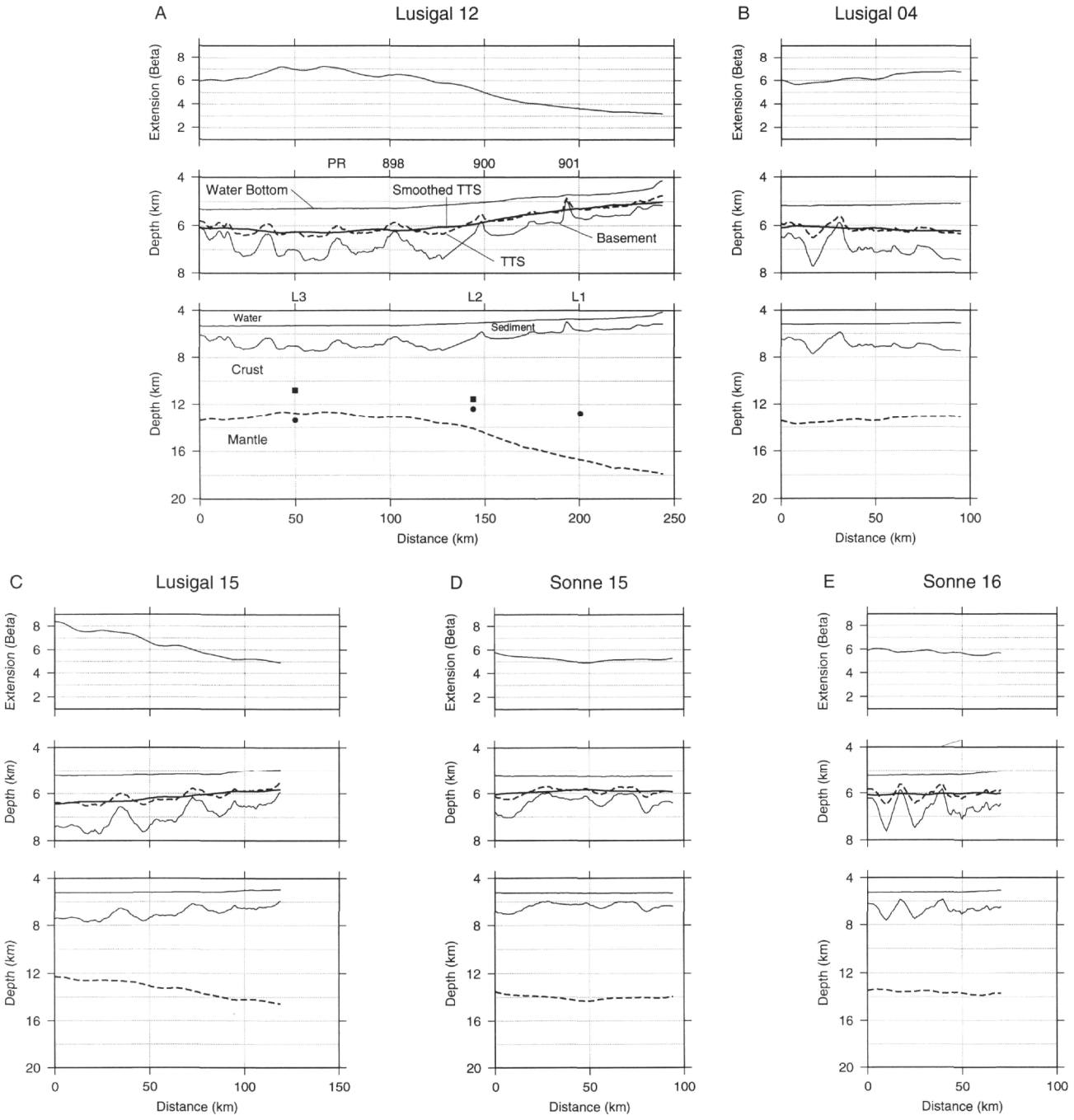

Figure 14. **A-L.** TTS, β, and estimated crustal cross sections along seismic profiles in the Iberia Abyssal Plain. We assume a rifting time of 135 Ma. The dashed curve in the lower plot is an estimate of the depth of the crust/mantle boundary based on an original crust thickness of 40 km and the β curve above. (A) The positions of the three seismic refraction lines (Whitmarsh et al., 1990b) L1, L2, and L3 are shown above the bottom panel. Below each are symbols indicating the depth to the contact between crust and serpentinized peridotite (squares), contact between serpentinized peridotite and mantle (circles for L2 and L3), and contact between crust and mantle (circle for L1). The positions of the Leg 149 sites and the peridotite ridge (PR) are annotated above the middle panel.

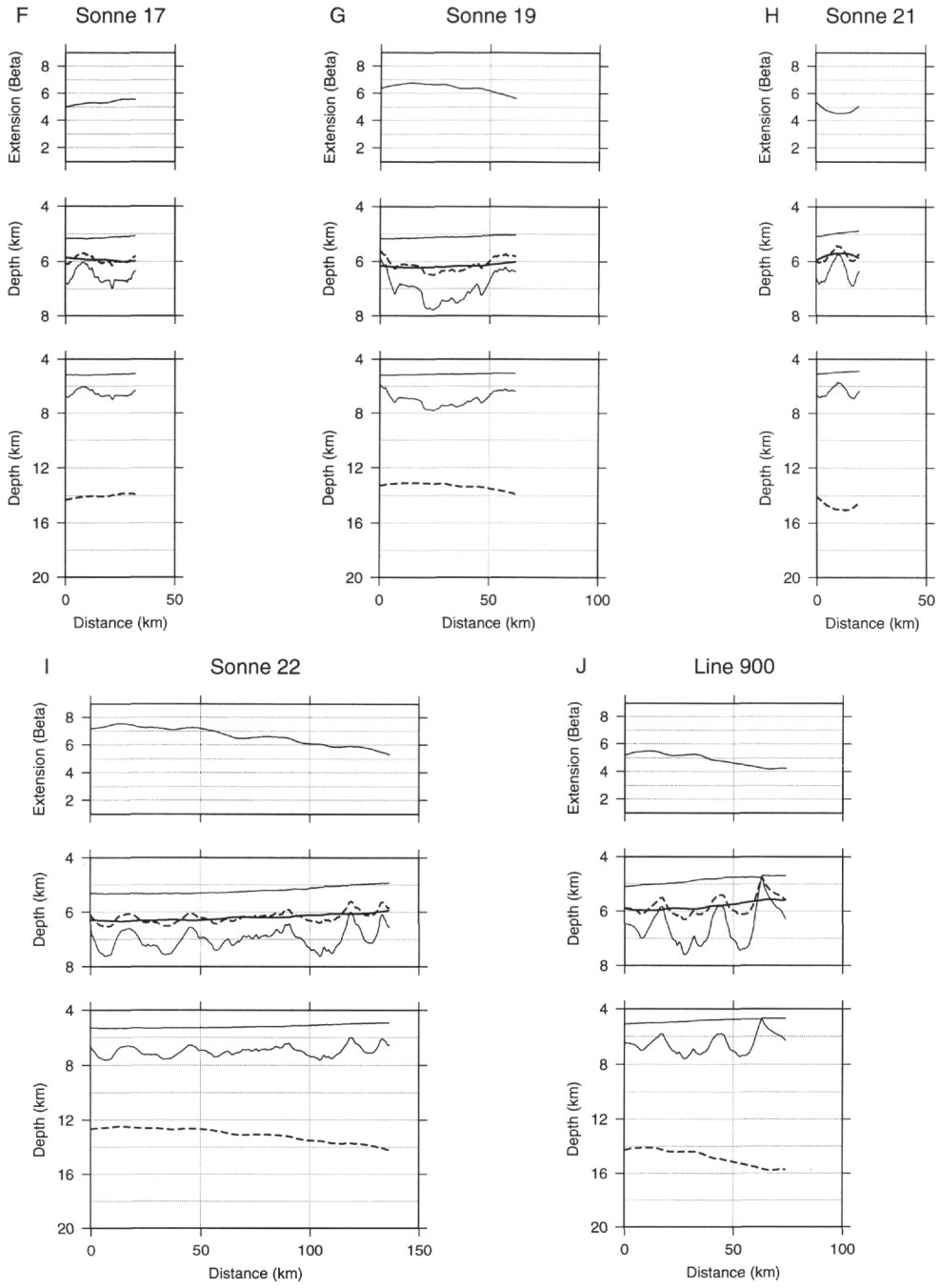

Figure 14 (continued).

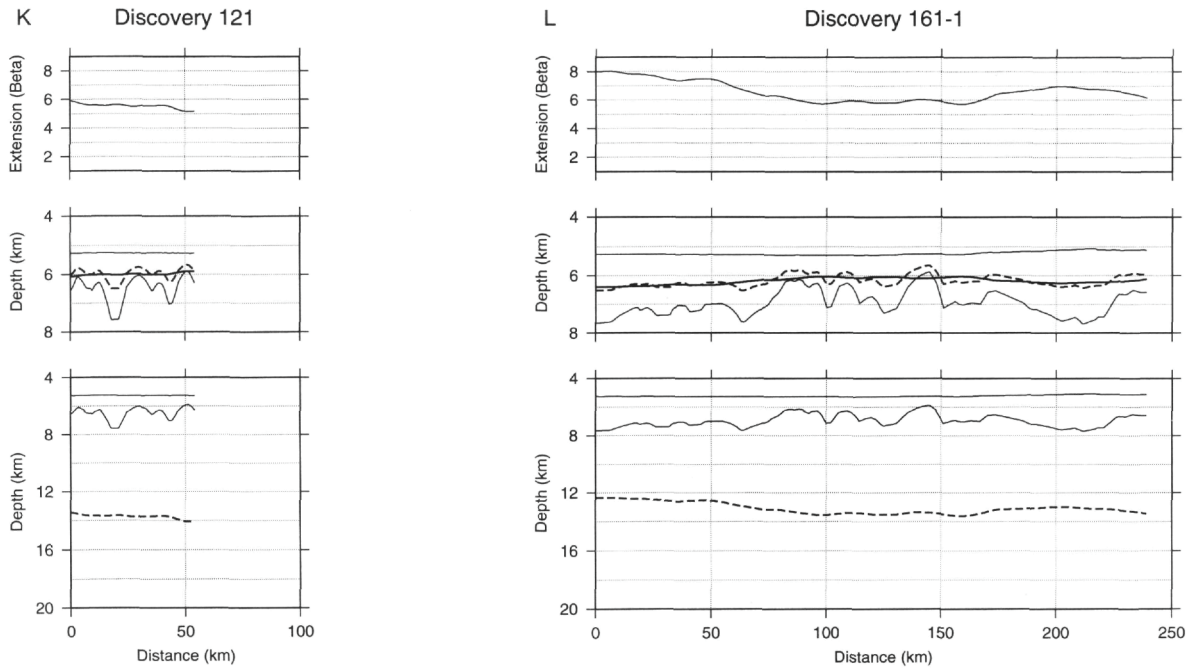

Figure 14 (continued).